JURNAL KIMIA VALENSI
p-ISSN: 2460-6065; e-ISSN: 2548-3013
Journal homepage: https://journal.uinjkt.ac.id/index.php/valensi
Research Article

Synthesis and Antibacterial Activity of Chitosan-Cinamaldehyde/AgNp Schiff Base Composite

Muhammad Badrul Huda[1], Kemilau Permata Hati Rinaryadi[1], Ngadiwiyana[1], Marcelinus Christwardana[1,2], Purbowatiningrum Ria Sarjono[1], Ismiyarto[1*]

[1]*Department of Chemistry, Faculty of Science and Mathematics, Diponegoro University, Semarang, 50275, Indonesia*
[2]*Master Program of Energy, School of Postgraduate Studies, Diponegoro University, Semarang, 50241, Indonesia*

[*]*Email: ismiyarto@lecturer.undip.ac.id*

Article Info
Received: Feb 25, 2025
Revised: June 3, 2025
Accepted: June 7, 2025
Online: June 17, 2025

Citation:
Huda, M. B., Rinaryadi, K. P. H., Ngadiwiyana., Christwardana, M., Sarjono, P. R., & Ismiyarto. (2025). Synthesis And Antibacterial Activity of Chitosan-Cinamaldehyde/AgNp Schiff Base Composite. *Jurnal Kimia Valensi*, 11(1), 126-137.

Doi: 10.15408/jkv.v11i1.45121

Abstract

Chitosan is a material that has antibacterial properties. Chitosan was modified with cinnamaldehyde to form chitosan Schiff base, which acts as a capping agent in the synthesis of silver nanoparticles. The Schiff base product was modified again into a silver nanoparticle Schiff base composite to improve its ability as a capping agent and improve its antibacterial properties. This study aims to synthesize a chitosan-cinnamaldehyde/AgNP Schiff base composite (CCSB/AgNP) as an active ingredient with excellent antibacterial properties. The first stage was the synthesis of a chitosan-cinnamaldehyde Schiff base. In the second stage, the synthesis of the chitosan/AgNP composite was carried out by adding STPP with sonication and a water bath. The third stage involved synthesizing of the CCSB/AgNP composite using the same method as the second stage employing both heating and non-heating as well as sonication and non-sonication. The product was characterized using a UV-Vis spectrophotometer, FT-IR, SEM-EDX, mapping, and AAS. Antibacterial tests were performed on the synthesized product using the Total Plate Count (TPC) method. Chitosan has a molecular weight of 338080 g/mol and a degree of deacetylation of 65.09%. The Schiff base product of chitosan-cinnamaldehyde is a brownish-yellow solid with a yield of 76.9% (w/w) and a degree of substitution of 87.02%. The presence of Ag was confirmed by EDX mapping, which revealed mass percentages of 0.26%, 1.00%, and 3.97% for C/AgNP-1, C/AgNP-2, and CCSB/AgNP-2, respectively. The chitosan/AgNP product has a yield of 97% (w/w) and an SPR effect at 439 nm. The synthesis of CCSB/AgNP obtained a dark green solid with a yield of 87% (w/w) and an SPR effect at 433 nm. The antibacterial activity test yielded the highest percentage reduction in the number of bacteria in CCSB/AgNP at 3 days of observation at 95.1%, and 7 days at 94.1%.

Keywords: Antibacterial, chitosan, nanoparticle Ag, Schiff base

1. INTRODUCTION

Chitosan is a material with antibacterial properties that can be used as a preservative to extend the shelf life of food products [1]. It exhibits antibacterial activity that can inhibit bacterial growth [2]. Chitosan is a linear polysaccharide polymer derived from the deacetylation of chitin, consisting of N-acetyl-2-amino-2-deoxy-D-glucose (glucosamine) and 2-amino-2-deoxy-D-glucose (N-acetylglucosamine) units. It can dissolve in aqueous acidic media due to the protonation of its primary amine groups [3]. Chitosan contains reactive groups, including primary amine groups ($–NH_2$) and primary and secondary hydroxyl groups (–OH) at positions C-2, C-3, and C-6 [4]. These functional groups allow for various modifications to enhance its antibacterial properties for food preservation, such as through the formation of Schiff bases. Efforts to preserve fresh chicken meat, which has a high nutrient and water content, are crucial due to its short shelf life and rapid quality degradation caused by spoilage microorganisms [5]. These microorganisms, commonly found on the meat's surface, degrade amino acids, oxidize lipids, and shorten the product's shelf life [6].

A Schiff base is synthesized through a condensation reaction between the primary amine

groups in chitosan and the carbonyl group of cinnamaldehyde. Cinnamaldehyde itself can be used as a food preservative [7]. The synthesis of a Schiff base from chitosan and cinnamaldehyde forms an imine group (C=N), which enhances antibacterial activity [8]. Further modifications of Schiff bases can increase their antibacterial properties and improve their ability to absorb silver (Ag) in the synthesis of silver nanoparticles (AgNPs) [9]. Silver nanoparticles are widely used due to their large surface area, which enhances microbial adsorption. Chitosan Schiff bases act as stabilizers in AgNP synthesis, preventing aggregation and agglomeration [10].

Previous studies have shown that chitosan modified with silver nanoparticles serves as a stable capping material, preventing agglomeration [11]. While previous studies have shown that chitosan modified with AgNPs serves as a stable capping material and prevents agglomeration, several research gaps remain. The long-term stability and effectiveness of chitosan-AgNP composites in real-world food preservation scenarios are not well understood. Additionally, the mechanisms behind their enhanced antibacterial properties need further investigation. There is also limited information on the potential toxicity and environmental impact of these composites. Addressing these gaps is crucial for developing safer and more effective chitosan-AgNP composites for food preservation applications.

In this study, we modified the synthesis of a chitosan-cinnamaldehyde/AgNP Schiff base composite using a method adapted from Badawy et al.. This composite exhibits excellent antibacterial properties as a preservative, which can extend the shelf life of chicken meat products [11]. The novelty of this research lies in the unique synthesis method and the application of the chitosan-cinnamaldehyde/AgNP Schiff base composite, which has not been previously reported. The synthesized and modified products will be characterized using UV-Vis spectrophotometry, FT-IR spectrophotometry, SEM-EDX analysis, mapping, and atomic absorption spectroscopy (AAS). The product will then be applied as a food preservative in chicken meat, with antibacterial efficacy tested using the Total Plate Count (TPC) method. The expected outcome is a chitosan-cinnamaldehyde/AgNP Schiff base with enhanced antibacterial properties and an optimized silver nanoparticle synthesis method.

2. RESEARCH METHODS

Materials and Instrumentation

The materials used in this study included chitosan (industrial grade, Chimultiguna), glacial acetic acid (Merck), cinnamaldehyde p.a. (Sigma-Aldrich), ethanol 96% (Jayamas Medical Industrial), acetone, $AgNO_3$ (Merck), ascorbic acid (Merck), sodium hydroxide (Merck), sodium tripolyphosphate (Merck), glycerol, distilled water, gelatin, NaCl (Merck), yeast, peptone (Merck), plate count agar (Merck), plastic wrap (Baguus), aluminum foil (Klin Pak). At the same time, chicken meat was purchased from local supermarket in Semarang.

The equipment and instruments used in this study included glassware (Herma), a magnetic stirrer (Corning PC-420D), magnetic bars, a Buchner funnel, an analytical balance (Ohaus Pioneer PA214 Analytical Balance), filter paper, a reflux apparatus set (Pyrex), an Ubbelohde viscometer, an oven (Binder), a water bath, a sonicator (Krisbow), an incubator, petri dishes (Herma), pH paper, an autoclave, tweezers, a spreader, a Laminar Air Flow Cabinet (Humanlab Limited Model T60u), a UV-Vis spectrophotometer (Thermo Scientific Genesys 10S UV-Vis), a Fourier transform infrared (FTIR) spectrophotometer (Perkin Elmer Spectrum IR 10.6.1), a Scanning Electron Microscope-Energy Dispersive X-ray Spectroscopy (SEM-EDX), and an atomic absorption spectrophotometer (AAS).

Synthesis of Chitosan-Cinnamaldehyde Schiff Base

The research procedure for synthesizing the chitosan-cinnamaldehyde Schiff base (CCSB) solution began by dissolving 5 g of chitosan (3.06 x 10^{-2} mol) in 250 mL of 3% acetic acid (v/v), followed by stirring with a magnetic stirrer for 60 minutes. Subsequently, 2.39 mL of cinnamaldehyde (1.9 x 10^{-2} mol) was added to 50 mL of 70% ethanol (v/v) and refluxed for 3 hours at 60°C. The mixture was then allowed to cool to room temperature, and the pH was checked. Precipitation was carried out by adding 5% NaOH (w/v) drop by drop until no more sediment formed, followed by filtration of the sediment using a Buchner funnel. The sediment was washed with distilled water until neutral pH was achieved, and then washed with 70% ethanol (v/v). The sediment was dried in an oven at 60°C until a constant mass was obtained. The product was weighed, and the synthesis results were characterized using UV-Vis and FTIR spectrophotometry [11].

Chitosan/AgNP Composite Synthesis

The synthesis of chitosan/AgNP (CA) composites was carried out using two methods that varied the step of STPP addition. The research procedure began by dissolving 2 g of chitosan in 100 mL of 1% (v/v) acetic acid solution. Then, 10 mL of 0.3% (w/v) $AgNO_3$ was added dropwise, followed by stirring with a magnetic stirrer for 30 minutes. Next, 10 mL of 1% (w/v) ascorbic acid was added dropwise until the pH reached 6, and the mixture was stirred for 1 h at 50 °C. Subsequently, 30 mL of 1% (w/v) STPP was added dropwise. Precipitation was carried out by

adding 1 N NaOH until the pH reached 12, followed by sonication for 15 minutes. The mixture was then evaporated using a water bath at 60 °C for 3 h. The precipitate was filtered using a Buchner funnel and washed with distilled water until a neutral pH was achieved. The precipitate was also washed with 70% ethanol (v/v). Finally, the precipitate was dried in an oven at 60°C until a constant mass was obtained, and the product was weighed[11]. The two methods differed in the timing of STPP addition: in the first method, STPP was added after Ag reduction with heating and sonication, while in the second method, STPP was added before Ag reduction with heating and sonication.

Synthesis of Chitosan-Cinnamaldehyde/AgNP Schiff Base Composite

The synthesis of chitosan-cinnamaldehyde/AgNP Schiff base (CCASB) composites was carried out using four methods, varying the steps of adding STPP, heating/non-heating, sonication/non-sonication, and water bath/non-water bath. The research procedure began by dissolving 2 g of the chitosan-cinnamaldehyde Schiff base compound in 100 mL of 1% (v/v) acetic acid solution. Then, 10 mL of 0.3% (w/v) $AgNO_3$ was added dropwise, followed by stirring with a magnetic stirrer for 30 minutes. Next, 10 mL of 1% (w/v) ascorbic acid was added dropwise until the pH reached 6, and the mixture was stirred for 1 hour at 50°C. Subsequently, 30 mL of 1% (w/v) STPP was added dropwise. Precipitation was carried out by adding 1 N NaOH until the pH reached 12, followed by sonication for 15 minutes. The mixture was then evaporated using a water bath at 60 °C for 3 h. The precipitate was filtered using a Buchner funnel and washed with distilled water until a neutral pH was achieved. The precipitate was also washed with 70% ethanol (v/v). Finally, the precipitate was dried in an oven at 60°C until a constant mass was obtained, and the product was weighed [11]. The four methods varied as follows: (i) adding STPP after Ag reduction with heating and sonication, (ii) adding STPP before Ag reduction with heating and sonication, (iii) adding STPP before Ag reduction, followed by stirring for 30 minutes without heating and sonication, (iv) adding STPP before Ag reduction without heating and sonication.

Antibacterial Test with Total Plate Count (TPC)

Antibacterial activity was tested using the Total Plate Count (TPC) method. Six active ingredients were prepared at two concentrations, 1000 ppm and 2500 ppm, each dissolved in 1% (v/v) acetic acid. The active ingredients included chitosan, chitosan-cinnamaldehyde Schiff base, chitosan/AgNP-1, chitosan/AgNP-2, chitosan-cinnamaldehyde Schiff base/AgNP-2, and chitosan-cinnamaldehyde Schiff base/AgNP-3. Additionally, a positive control solution (ciprofloxacin) and a negative control solution (1% acetic acid) were prepared.

Characterization of Chitosan/AgNP Derivative Composites

Characterization was conducted to determine the physical and chemical properties of chitosan/AgNP derivative products, including maximum wavelength, SPR phenomenon, wave number, molecular weight, particle size, and element distribution. The characterization of chitosan/AgNP and CCSB/AgNP products was performed using UV-Vis spectrophotometry, FT-IR spectroscopy, SEM-EDX, mapping, and spectroscopy.

3. RESULTS AND DISCUSSION

Identification of Chitosan

Identification of chitosan was performed by determining its molecular weight (MW) and degree of deacetylation (DD). The molecular weight of chitosan was determined using an Ubbelohde viscometer and the Mark-Houwink equation. The molecular weight of chitosan was found to be 338,080 g/mol, corresponding to 2,086 monomer units. The degree of deacetylation (DD) of chitosan was determined using an FTIR spectrophotometer within the wavenumber range of 4000-400 cm^{-1}, employing the baseline method. The DD was calculated to be 65.09%, indicating the presence of free amine groups replacing the acetyl groups. Based on **Figure 1**, there is an absorption peak at wave number 3354 cm^{-1}, which is the stretching vibration of the –OH and $–NH_2$ groups. The absorption at wave number 2877 cm^{-1} is the aliphatic C_{sp3}–H stretching vibration, while the absorption at wave number 1647 cm^{-1} is the C=O stretching vibration of the chitosan acetyl group [12].

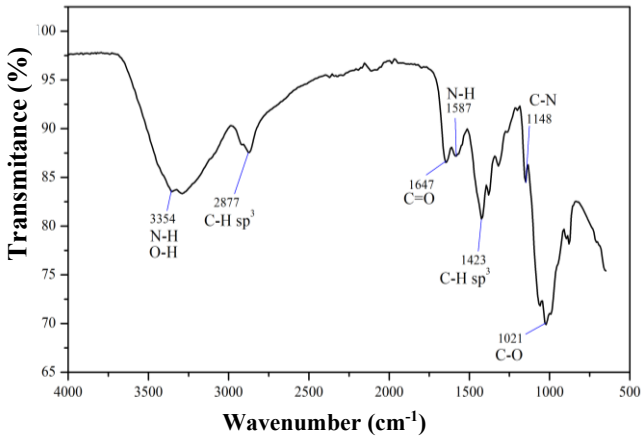

Figure 1. FTIR spectra of chitosan

Synthesis of Chitosan-Cinnamaldehyde Schiff Base

Figure 2 illustrates the Schiff base formation between chitosan and cinnamaldehyde, a reaction widely explored in biopolymer modifications for

biomedical and antimicrobial applications. Chitosan reacts with cinnamaldehyde to produce a chitosan-cinnamaldehyde Schiff base as the synthesis product. The Schiff base compound has an imine group (>C=N–) formed due to the primary amine group from chitosan reacting with the carbonyl group of cinnamaldehyde through a condensation reaction. In this reaction, the primary amine group in chitosan acts as a nucleophile, while the carbonyl group in cinnamaldehyde acts as an electrophile [13]. The synthesis results in a brownish-yellow solid product using 1355 cinnamaldehyde monomers, with a yield of 76.9% (w/w). The degree of substitution (DS) of 87.02% reported in the figure indicates a high conversion rate of chitosan's amine groups into Schiff base structures, suggesting efficient reaction conditions.

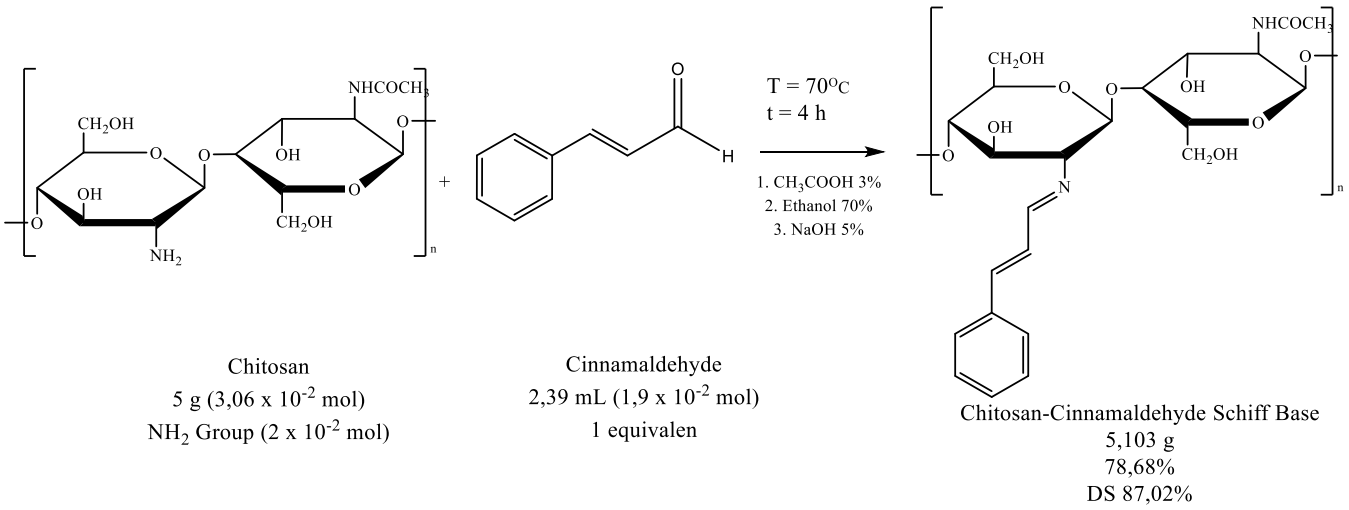

Figure 2. Mechanism of formation Schiff base

Figure 3 presents the UV-Vis absorption spectra of chitosan, cinnamaldehyde, and the Schiff base product of chitosan-cinnamaldehyde (CCSB), providing insights into the electronic transitions and structural modifications occurring upon Schiff base formation. Upon Schiff base formation, the UV-Vis spectrum of chitosan-cinnamaldehyde (CCSB) exhibits notable shifts, confirming the successful formation of the imine (-C=N-) bond. The absorption peak at 229 nm corresponds to the π→π* transition of the benzene ring conjugated with the imine group, indicating an extension of conjugation due to Schiff base formation. More importantly, the appearance of a new absorption band at 292 nm represents the π→π* transition of the C=N bond conjugated with the benzene ring, confirming the successful modification of chitosan with cinnamaldehyde. This shift to a higher wavelength (red shift) suggests an increase in conjugation within the molecular structure, making the electronic transitions more efficient and indicating the presence of a more extended π-system.

The observed spectral shifts provide strong evidence for Schiff base formation, as the conversion of the aldehyde (-CHO) functional group into an imine (-C=N-) alters the electron distribution in the molecule. The increase in absorbance intensity and shift towards longer wavelengths highlight the enhanced delocalization of electrons, which stabilizes the structure and modifies its optical properties. These results confirm that the Schiff base formation not only modifies the chemical structure but also impacts its electronic and photophysical properties, making it a valuable material for potential applications in antimicrobial agents, metal chelation, and sensor development [14].

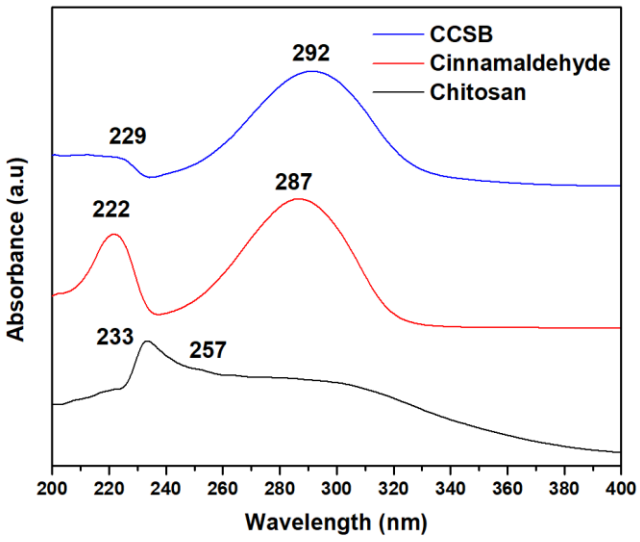

Figure 3. UV-Vis spectra of chitosan-cinnamaldehyde Schiff base, chitosan, and cinnamaldehyde

Characterization was carried out using an FTIR spectrophotometer on chitosan-cinnamaldehyde Schiff base products. The FTIR spectra of chitosan-cinnamaldehyde Schiff base were compared with

chitosan. **Figure 4** shows the FT-IR spectra, which illustrate the structural differences between chitosan and its Schiff base derivative with cinnamaldehyde (CCSB) by comparing their functional group vibrations. The transformation of chitosan into the Schiff base is confirmed by notable shifts in key absorption bands, particularly in the region associated with carbonyl (C=O) and imine (C=N) functional groups. In the spectrum of pure chitosan (red), a characteristic absorption band at 1647 cm^{-1} corresponds to the carbonyl (C=O) stretching vibration, which is attributed to the residual acetyl groups in chitosan. However, in the Schiff base product (black), this peak is replaced by a new band at 1632 cm^{-1}, confirming the formation of the imine (-C=N-) functional group through a condensation reaction between the amine ($-NH_2$) groups of chitosan and the aldehyde (-CHO) groups of cinnamaldehyde[15].

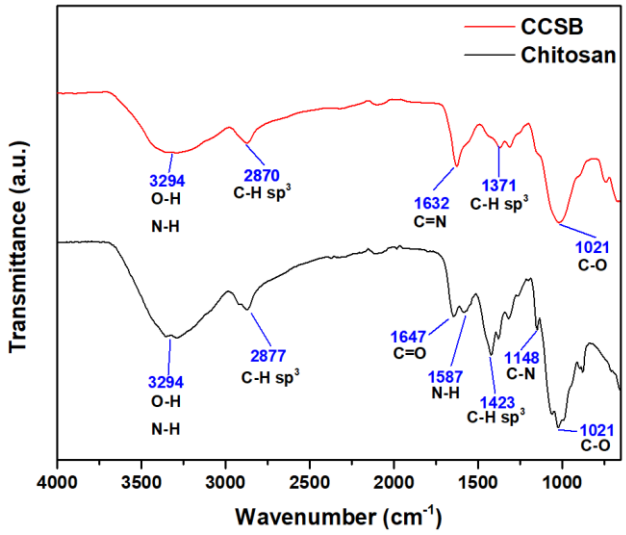

Figure 4. FTIR spectra of chitosan and chitosan-cinnamaldehyde Schiff base

Synthesis of Chitosan/AgNP Derivative Composite

Chitosan derivatives (chitosan and chitosan-cinnamaldehyde Schiff base) are reacted with $AgNO_3$ and ascorbic acid to form a silver nanoparticle chitosan composite. **Table 1** provides comparative data on the synthesis of silver nanoparticle (AgNP) composites with chitosan and its Schiff base derivative (CCSB) using different preparation methods. The synthesis was varied using four methods. In the first method, STPP was added after Ag reduction, with heating and sonication. The second method involved adding STPP before Ag reduction, with heating and sonication. The third method used a two-fold $AgNO_3$ ratio, with STPP added before Ag reduction, and the mixture was stirred for 30 minutes without heating or sonication. The fourth method also used a double $AgNO_3$ ratio, with STPP added before Ag reduction, without heating or sonication.

The yields of chitosan/AgNP-1 and chitosan/AgNP-2 were 83.4% (w/w) and 80.8% (w/w), respectively, with dark brownish-yellow and yellow-brown solid colors. The yields of CCSB/AgNP-1, CCSB/AgNP-2, CCSB/AgNP-3, and CCSB/AgNP-4 were 80.8% (w/w) with a dark green solid color, 75.3% (w/w) with a brownish-green solid color, 74.3% (w/w) with a dark green solid color, and 41.5% (w/w) with a light green solid color, respectively (**Figure 6**). The SPR effect was observed at 420 nm for chitosan/AgNP-1 and at 439 nm for chitosan/AgNP-2. CCSB/AgNP-1 and CCSB/AgNP-3 did not exhibit SPR effects, while CCSB/AgNP-2 showed an SPR effect at 433 nm and CCSB/AgNP-4 at 445 nm. Literature indicates that the formation of Ag nanoparticles is typically observed in the 350 to 450 nm band [16]. A blue shift (shift to a shorter wavelength) indicates a smaller nanoparticle size, and a sharper peak suggests a more uniform nanoparticle size[17].

Table 1. Preparation of composite chitosan-derivatives/AgNP

Sample	Method	Product	Yield (%)	SPR Effect (nm)	ε ($cm^2\ g^{-1}$)	Peak profile	Ag adsorbed (%)
Chitosan	I	C/AgNP-1	83,4	420	664	Sharp	2,86
Chitosan	II	C/AgNP-2	80,8	439	598	Very Sharp	1,91
CCSB	I	CCSB/AgNP-1	72,3	-	-	-	-
CCSB	II	CCSB/AgNP-2	75,3	433	130	little sharp	2,14
CCSB	III	CCSB/AgNP-3	74,3	-	-	-	1,52
CCSB	IV	CCSB/AgNP-4	41,5	445	95	Very weak	-

extinction coefficient (ε); CCSB = chitosan-cinnamaldehyde Schiff base; C/AgNP = chitosan/AgNP; CCSB/AgNP = chitosan-cinnamaldehyde Schiff base/AgNP.

The results indicate that the second method for synthesizing the chitosan/AgNP composite is superior to the first method. This is evident from the higher peak observed in chitosan/AgNP-2, which is attributed to the different steps involved in the addition of STPP. In the second method, STPP is added before the reduction of Ag to nanoparticles, allowing chitosan and CCSB to react first with STPP, producing a more hollow and organized structure. This facilitates better and more organized distribution of Ag nanoparticles. The reduction process of Ag^+ to Ag^0 is more uniform, resulting in more uniform particle sizes [18].

For the CCSB/AgNP composite, the second synthesis method also yielded the best results. CCSB/AgNP-1 and CCSB/AgNP-3 did not exhibit sharp SPR peaks, indicating that silver nanoparticles were not formed due to insufficient contact with the reducing agent. Adding STPP before Ag reduction enhances the ability of CCSB as a capping agent, making it more hollow and stable in arranging Ag metal. Sonication improves the stability of polydispersity and even distribution of Ag nanoparticle size, preventing agglomeration [19].

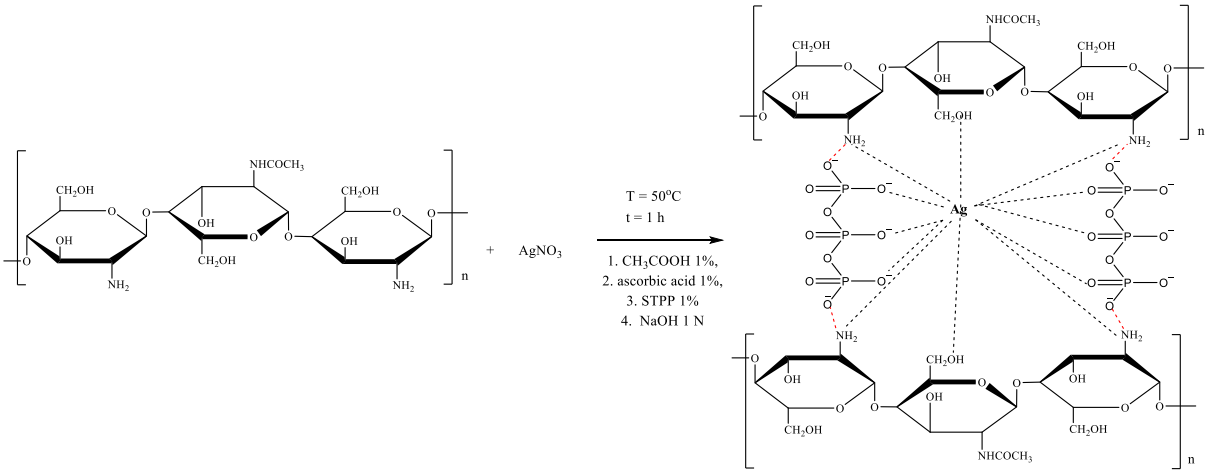

Figure 5. Reaction mechanism of formation composite chitosan/AgNP

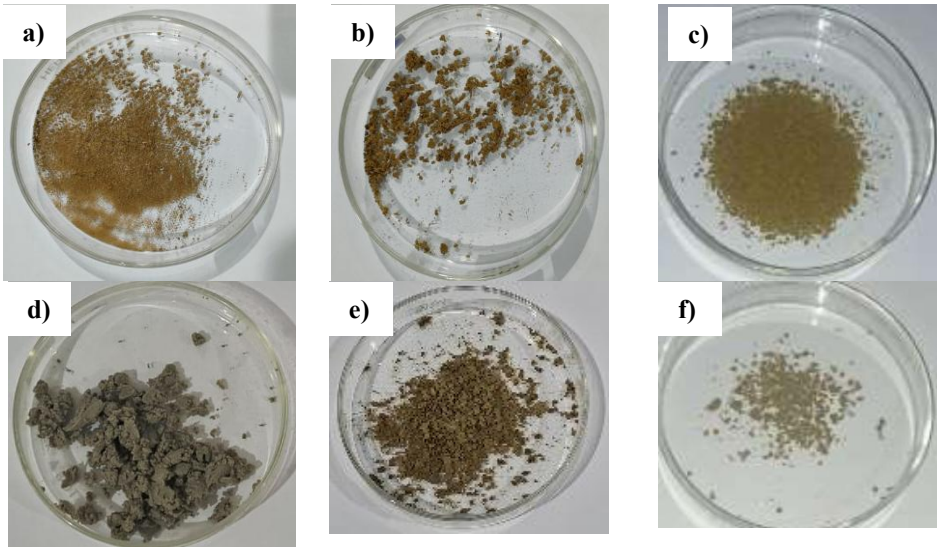

Figure 6. Synthesis products of chitosan/AgNP derivative composites; a) chitosan/AgNP-1, b) chitosan/AgNP-2, c) CCSB/AgNP-1, d) CCSB/AgNP-2, e) CCSB/AgNP-3, f) CCSB/AgNP-4

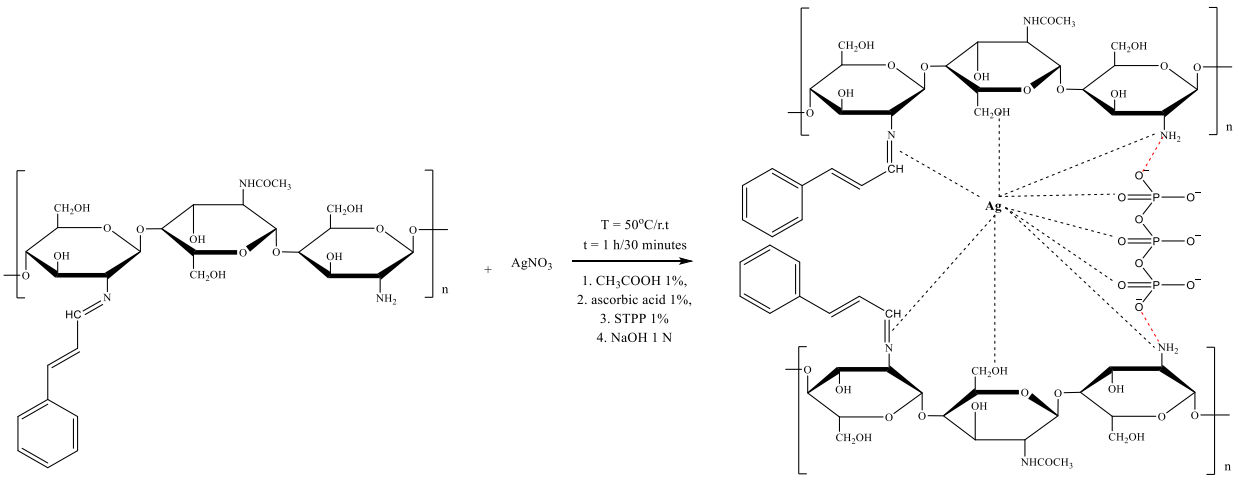

Figure 7. Reaction mechanism of formation composite chitosan-cinnamaldehyde Schiff base/AgNP

SEM-EDX Characterization

The SEM analysis of chitosan/AgNP composites was conducted to evaluate the surface morphology and Ag nanoparticle distribution within the matrix. The micrographs in **Figure 8** provide insights into the impact of different synthesis methods on nanoparticle formation and dispersion. The size that can be categorized as nanoparticles ranges from 1 to 100 nm. SEM characterization will reveal the surface morphology of chitosan/AgNP which contains nanoparticles. The second method of chitosan/AgNP, namely the method with the addition of STPP at the beginning, showed that it had the smallest average particle size with an average diameter of 32.195 nm, while the first method of chitosan/AgNP showed that it had a larger average particle size with an average diameter of 99.131 nm.

The elemental composition analysis of chitosan and chitosan/AgNP composites, as shown in **Table 2**, provides valuable insights into the structural modifications and silver nanoparticle (AgNP) incorporation in different samples. Chitosan, as the base material, consists mainly of carbon (C), nitrogen (N), and oxygen (O), with no detectable silver (Ag). In the C/AgNP-1 sample, a small amount of Ag (0.26%) is detected, suggesting a relatively low incorporation of silver nanoparticles. A more significant increase in Ag content is observed in the C/AgNP-2 sample, reaching 1.00%. The Schiff base chitosan-cinnamaldehyde composite loaded with AgNPs (CCSB/AgNP-2) exhibits the highest Ag content (3.97%), which is significantly greater than both C/AgNP-1 and C/AgNP-2.

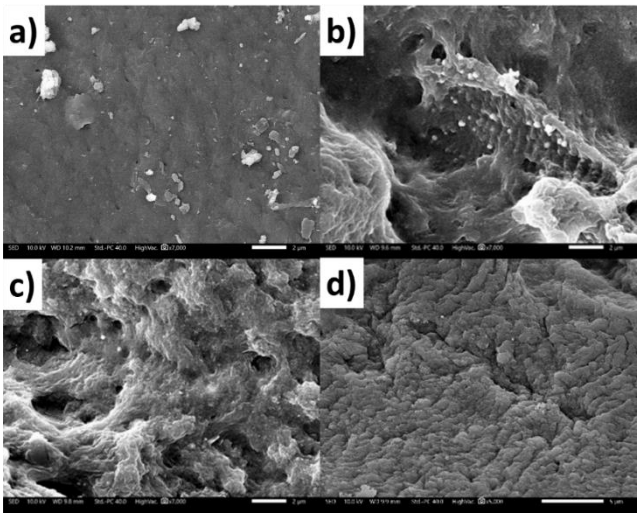

Figure 8. Surface morphology under 7000x magnification of chitosan (a), chitosan/AgNP-1 (b), chitosan/AgNP-3 (c), and CCSB/AgNP-2 (d)

Table 2. Mass percentage of chitosan/AgNP-1 and chitosan/AgNP-2

Element	Sample			
	Chitosan	C/AgNP-1	C/AgNP-2	CCSB/AgNP-2
	%Mass	%Mass	%Mass	%Mass
C	44.06	44.03	43.33	57.40
N	9.93	10.37	9.67	4.99
O	46.00	45.34	46.01	33.64
Ag	-	0.26	1.00	3.97
Total	100.00	100.00	100.00	100.00

C/AgNP = chitosan/AgNP

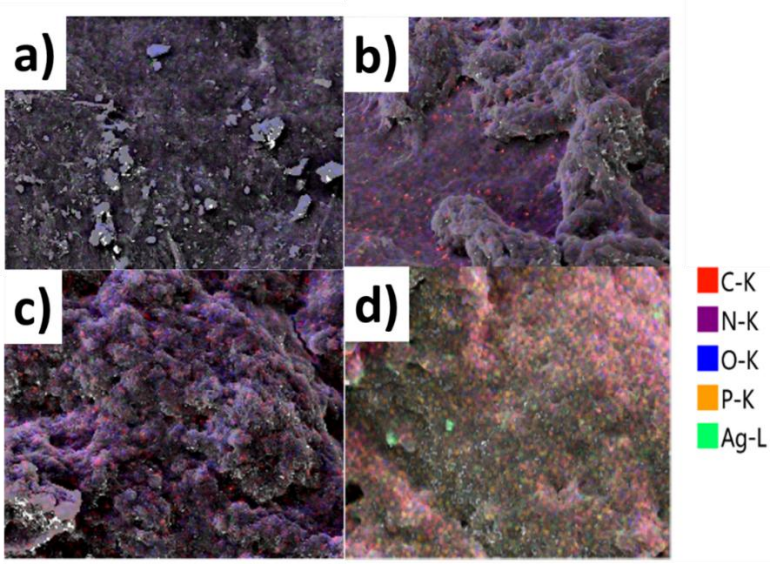

Figure 9. Mapping of chitosan (a), chitosan/AgNP-1 (b), chitosan/AgNP-2 (c), and CCSB/AgNP-2 (d)

The mapping analysis provides crucial insights into the distribution of silver (Ag) within the chitosan and its modified composite structures. **Figure 9a** represents pure chitosan, showing a lack of silver, as expected, and demonstrating a relatively homogeneous structure composed primarily of carbon (C), nitrogen (N), and oxygen (O). In contrast, **Figure 9b** displays chitosan/AgNP-1, where silver nanoparticles (AgNPs) are present but appear in a more clustered and non-uniform manner. In **Figure 9c**, chitosan/AgNP-2 exhibits a noticeably more even dispersion of silver compared to chitosan/AgNP-1. This improved distribution can be attributed to the addition of STPP prior to Ag reduction. STPP acts as a crosslinking agent, interacting with chitosan's functional groups to create a more open and organized polymeric network. The most uniform Ag dispersion is observed in **Figure 9d**, which corresponds to CCSB/AgNP-2. This sample, which involves Schiff base modification of chitosan with cinnamaldehyde before AgNP incorporation, exhibits the most effective Ag distribution. The mapping image confirms the successful integration of AgNPs within CCSB/AgNP-2, as indicated by the well-distributed green (Ag-L) signals. This result suggests that the Schiff base modification enhances the affinity of chitosan for silver, ensuring superior nanoparticle immobilization.

Characterization of UV-Vis Spectrophotometer

The UV-Vis spectrophotometry analysis of chitosan/AgNP composites and Schiff base-modified chitosan-cinnamaldehyde/AgNP composites provides significant insights into the formation and distribution of AgNPs within the polymer matrix. The surface plasmon resonance (SPR) phenomenon observed in the spectra serves as a crucial indicator of AgNP formation, with characteristic peaks typically appearing in the 350–450 nm range[20]. The precise position, shape, and intensity of these peaks provide valuable information regarding the size, uniformity, and dispersion of the nanoparticles within the composite material[21].

In **Figure 10a**, the spectra for chitosan/AgNP-1 and chitosan/AgNP-2 show distinct SPR peaks at 420 nm and 439 nm, respectively. The peak at 420 nm in chitosan/AgNP-1 suggests the presence of AgNPs with a relatively smaller particle size. However, the broad peak profile indicates a heterogeneous size distribution, likely due to nanoparticle aggregation resulting from an insufficient stabilization mechanism during the synthesis process. On the other hand, chitosan/AgNP-2 exhibits a red-shifted SPR peak at 439 nm, suggesting a larger nanoparticle size compared to chitosan/AgNP-1[21]. **Figure 10b** illustrates the SPR spectra for CCSB/AgNP composites, which involve Schiff base-modified chitosan. The observed peaks at 433 nm (CCSB/AgNP-2) and 445 nm (CCSB/AgNP-4) indicate the successful incorporation of silver nanoparticles into the Schiff base-chitosan framework. The peak at 433 nm in CCSB/AgNP-2 suggests a relatively well-distributed and moderately sized nanoparticle population, whereas the peak at 445 nm in CCSB/AgNP-4 signifies a further increase in particle size.

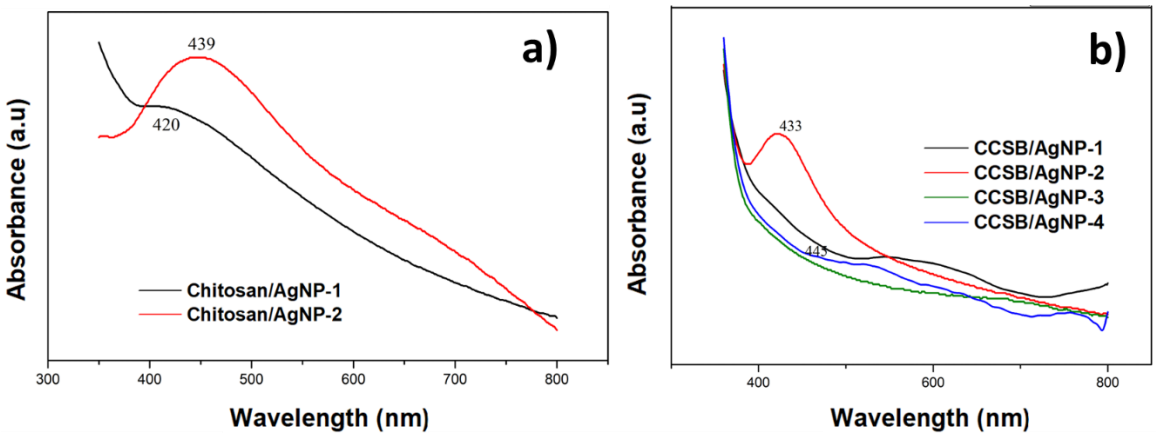

Figure 10. Comparison UV-Vis spectra of composite a) Chitosan/AgNP products, and b) Chitosan-cinnamaldehyde Schiff base products

FTIR Spectrophotometer Characterization

The FTIR spectra results reveal that the bands from chitosan/AgNP are not as broad and sharp as those of pure chitosan (**Figure 11a**). This suggests a reduction in bonding interactions due to the presence of Ag nanoparticles[22]. The hydroxyl (-OH) and amine (-NH_2) groups in chitosan, which typically absorb at 3354 cm^{-1}, shift to 3294 cm^{-1} in chitosan/AgNP, indicating interactions between the primary amines and silver nanoparticles[22]. A further shift is observed in CCSB/AgNP, where the -OH and -NH2_22 stretches move from 3294 cm^{-1} to 3284 cm^{-1}, suggesting additional modifications due to Schiff base formation (**Figure 11b**). The presence of aliphatic C—

H stretching vibrations at 2877 cm^{-1} in chitosan/AgNP and 2870 cm^{-1} in CCSB demonstrates that the aliphatic structure remains unchanged mainly but may experience slight modifications due to molecular interactions. Additionally, in the Schiff base-modified samples, the characteristic carbonyl (C=O) stretching vibration at 1647 cm^{-1}, commonly seen in chitosan, disappears. Instead, a new peak appears at 1632 cm^{-1} in CCSB, shifting slightly to 1630 cm^{-1} in CCSB/AgNP. This confirms the successful formation of imine (C=N) bonds, a hallmark of Schiff base modification, and their interaction with AgNPs.

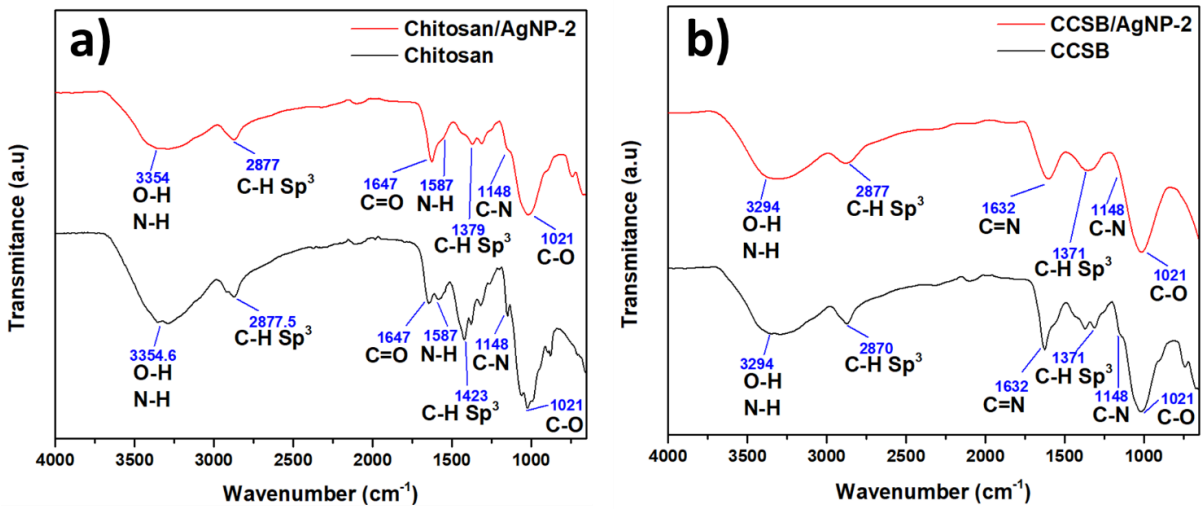

Figure 11. Comparison FTIR spectra of a) Chitosan and chitosan/AgNP composite, while b) Chitosan-cinnamaldehyde Schiff base and chitosan-cinnamaldehyde Schiff base/AgNP composite

Table 3. Data interpretation FTIR spectra of chitosan/AgNP and chitosan-cinnamaldehyde Schiff base/AgNP

Wavenumber (cm^{-1})				Functional Group Vibration
C	C/AgNP	CCSB	CCSB/AgNP	
3354	3294	3294	3284	Stretching –OH and $–NH_2$
2877	2877	2870	2877	Stretching C_{sp3}—H aliphatic
1647	1647	-	-	Stretching C=O
-	-	1632	1630	Stretching C=N
1587	1587	-	-	Bending N—H
1423	1379	1371	1371	Bending C_{sp3}—H aliphatic
1148	1148	1148	1148	Stretching C—N
1021	1028	1021	1021	Stretching C—O

C = chitosan; C/AgNP = chitosan/AgNP; CCSB = chitosan-cinnamaldehyde Schiff base; CCSB/AgNP = chitosan-cinnamaldehyde Schiff base/AgNP

Table 4. Silver content in chitosan/AgNP and chitosan-cinnamaldehyde Schiff base/AgNP

Sample	SPR (nm)	Concentration (ppm)	Ag mass in 1 g (mg)	Ag adsorbed
Chitosan/AgNP-1	420	0,6799	0,0679	2,86%
Chitosan/AgNP-2	439	0,4537	0,0453	1,91%
CCSB/AgNP-2	433	0,4916	0,0492	2,14%
CCSB/AgNP-3	-	0,3498	0,0349	1,52%

CCSB/AgNP = chitosan-cinnamaldehyde Schiff base/AgNP

Atomic Absorption Spectroscopy (AAS) Characterization

Atomic Absorption Spectroscopy (AAS) characterization is utilized to quantify the silver (Ag) content in the synthesized chitosan-based and Schiff-base chitosan-cinnamaldehyde-based AgNP composites. From the AAS data in **Table 4**, the difference in Ag content between chitosan/AgNP-1 and chitosan/AgNP-2 with CCSB/AgNP-2 and CCSB/AgNP-3 was obtained due to the difference in the synthesis method used. The difference in the synthesis method resulted in a difference in the total Ag content that entered the compound. It can be concluded that the CCSB/AgNP-2 and chitosan/AgNP-1 can absorb Ag better than the CCSB/AgNP-3 and chitosan/AgNP-2. In addition, the synthesis method of CCSB/AgNP-2 is better than CCSB/AgNP-3 because it can produce Ag that is more stable in undergoing reduction due to the heating and sonication process and can interact with chitosan-cinnamaldehyde Schiff base better[23].

Antibacterial Activity Test

The antibacterial activity of chitosan/AgNP composite and the chitosan-cinnamaldehyde/AgNP Schiff base was tested using the Total Plate Count (TPC) method, as shown in **Figure 12**. The interaction between chitosan-cinnamaldehyde Schiff base and chitosan with silver nanoparticles occurs because both chitosan and chitosan-cinnamaldehyde Schiff base can absorb silver ions through chelation and ion exchange mechanisms[24]. The larger surface area of silver nanoparticles enhances their antibacterial ability due to their interaction with chitosan and chitosan-cinnamaldehyde Schiff base, which prevents aggregation of AgNPs[25]. If agglomeration occurs, the surface area of AgNPs decreases, significantly reducing their antibacterial efficiency.

The mechanism of chitosan and chitosan-cinnamaldehyde Schiff base involves interaction with the bacterial cell membrane. Chitosan forms cations on the ammonium group (NH_3^+), which has a positive charge and can interact with negatively charged lipopolysaccharides on the bacterial cell surface[26]. The antibacterial mechanism of chitosan-based silver nanoparticles and chitosan-cinnamaldehyde Schiff base is enhanced because they release silver ions from their particles, which can enter bacterial cells[27]. Initially, AgNPs penetrate the bacterial cell membrane, producing Reactive Oxygen Species (ROS) that cause oxidative stress and damage various cell components[28]. The chitosan-cinnamaldehyde Schiff base/AgNP-2 composite showed a percentage reduction in the bacterial count of 95.1% on day 3 and 94.1% on day 7. These results indicate that the composite with silver nanoparticles has effective antibacterial properties.

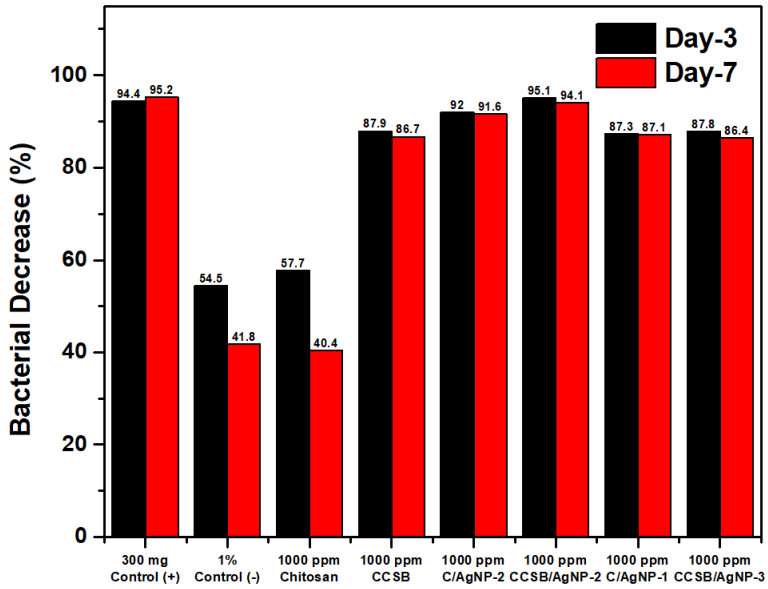

Figure 12. Percentage reduction of total bacterial colonies graphic

4. CONCLUSIONS

In conclusion, the study successfully synthesized a chitosan-cinnamaldehyde/AgNP Schiff base composite (CCSB/AgNP) with enhanced antibacterial properties. The multi-stage synthesis process, involving the formation of a chitosan-cinnamaldehyde Schiff base, a chitosan/AgNP composite, and a CCSB/AgNP composite, demonstrated effective methodologies for producing stable and efficient antibacterial agents. The synthesis of CCSB produced a brownish-yellow solid with a yield of 76.9% (w/w) and a degree of substitution of 87.02%. The best synthesis of chitosan/AgNP-2 resulted in a brownish-yellow solid with a yield of 80.8% (w/w) and an SPR phenomenon at 439 nm. Similarly, the best synthesis of CCSB/AgNP-2 yielded a darker green solid with a yield of 75.3% (w/w) and an SPR phenomenon at 433 nm. Characterization techniques, including UV-Vis spectrophotometry, FT-IR spectroscopy, SEM-EDX analysis, mapping, and AAS, confirmed the structural and compositional integrity of the synthesized products. Antibacterial tests revealed significant reductions in bacterial counts, particularly with CCSB/AgNP-2, which achieved a 95.1% reduction at 3 days and 94.1% at 7 days. These findings highlight the potential of CCSB/AgNP composites as promising antibacterial agents for various applications.

ACKNOWLEDGMENTS

This project is fully supported by “Sumber Dana Selain APBN UNDIP_Tahun 2023-RISET PUBLIKSI INTERNASIONAL”., with assignment letter No.569-109/UN7.D2/PP/V/2023.

REFERENCES

1. Ramezani Z, Zarei M, Raminnejad N. Comparing the effectiveness of chitosan and

nanochitosan coatings on the quality of refrigerated silver carp fillets. *Food Control.* 2015;51:43-48. https://doi.org/10.1016/j.foodcont.2014.11.015
2. Yilmaz H. Antibacterial activity of chitosan-based systems. *Functional chitosan: drug delivery and biomedical applications.* 2019:457-489. doi: 10.1007/978-981-15-0263-7_15
3. Aranaz I, Alcántara AR, Civera MC, Arias C, Eloza B, Caballero AH, Acosta N. Chitosan: An overview of its properties and applications. *Polymers.* 2021;13(19):3256. doi: 10.3390/polym13193256
4. Zhang J, Xia W, Liu P, Cheng Q, Tahirou T, Gu W, Li B. Chitosan modification and pharmaceutical/biomedical applications. *Marine drugs.* 2010;8(7):1962-1987. doi: 10.3390/md8071962
5. Ntzimani A, Kalamaras A, Tsironi T, Taoukis P. Shelf Life Extension of Chicken Cuts Packed under Modified Atmospheres and Edible Antimicrobial Coatings. *Applied Sciences.* 2023;13(6):4025. https://doi.org/10.3390/app13064025
6. Rouger A, Tresse O, Zagorec M. Bacterial contaminants of poultry meat: sources, species, and dynamics. *Microorganisms.* 2017;5(3):50. doi: 10.3390/microorganisms5030050
7. Qu S, Yang K, Chen L, et al. Cinnamaldehyde, a promising natural preservative against Aspergillus flavus. *Frontiers in microbiology.* 2019;10:2895. doi: 10.3389/fmicb.2019.02895
8. Antony R, Arun T, Manickam STD. A review on applications of chitosan-based Schiff bases. *International journal of biological macromolecules.* 2019;129:615-633. doi: 10.1016/j.ijbiomac.2019.02.047
9. Fontana R, Marconi PCR, Caputo A, Gavalyan VB. Novel chitosan-based Schiff base compounds: chemical characterization and antimicrobial activity. *Molecules.* 2022;27(9):2740. doi: 10.3390/molecules27092740
10. Alharthi SS, Gomathi T, Joseph JJ, Rakshavi J, Florence JAK, Sudha PN, Rajakumar G, Thiruvengadam M. Biological activities of chitosan-salicylaldehyde schiff base assisted silver nanoparticles. *Journal of King Saud University-Science.* 2022;34(6):102177. doi: 10.1016/j.jksus.2022.102177
11. Badawy ME, Lotfy TM, Shawir S. Preparation and antibacterial activity of chitosan-silver nanoparticles for application in preservation of minced meat. *Bulletin of the National Research Centre.* 2019;43(1):1-14. https://doi.org/10.1186/s42269-019-0124-8
12. Hisbiyah A, Fadhilah LN, Hidayah R. Antibacterial Activity of Sugarcane Bagasse Nanocellulose Biocomposite with Chitosan Against Escherichia coli. *Jurnal Kimia Valensi.* 2021, 7(1) 28-37. doi: 10.15408/jkv.v7i1.18718
13. Emriye A. Synthesis and Characterization of Schiff Base 1-Amino-4-methylpiperazine Derivatives. *Celal Bayar University Journal of Science.* 2016;12(3):375-392. https://doi.org/10.18466/cbayarfbe.280600
14. Iversen LJL, Mariah AMA, Nasir MN, Joseph MV, Wen XLF and Kobun R. Physicochemical Characterization and Antimicrobial Analysis of Vegetal Chitosan Extracted from Distinct Forest Fungi Species. *Polymers*. 2023, 15, 2328.https://doi.org/10.3390/polym15102328
15. Mousavi Z, Babaei S, Naseri M, Hosseini SMH, Shekarforoush SS. Utilization in situ of biodegradable films produced with chitosan, and functionalized with ε-poly-l-lysine: An effective approach for super antibacterial application. *Journal of Food Measurement and Characterization.* 2022;16(2):1416-1425. https://doi.org/10.1007/s11694-022-01297-2
16. Hussain I, Ullah A, Khan AU, Khan WU, Ullah R, Abdelaaty A, Almoqbil S, Naser, Mahmood HM. Synthesis, characterization and biological activities of hydrazone schiff base and its novel metals complexes. *Sains Malays.* 2019;48(7):1439-1446. doi: 10.17576/jsm-2019-4807-13
17. Yusniar Y, Hindryawati N, Ruga R. Sintesis Nanopartikel Perak Menggunakan Reduktor Asam Askorbat. Prosiding Seminar Nasional Kimia [S.l.], p. 187-192, oct. 2021.
18. Badi'ah HI. Chitosan as a capping agent of silver nanoparticles. *Indonesian Journal of Chemical Research.* 2021;9(1):21-25. https://doi.org/10.30598/ijcr.2021.9-han
19. Padman AJ, Henderson J, Hodgson S, Rahman PK. Biomediated synthesis of silver nanoparticles using Exiguobacterium mexicanum. *Biotechnology letters.* 2014;36:2079-2084. doi: 10.1007/s10529-014-1579-1
20. Ider M, Abderrafi K, Eddahbi A, Ouaskit S, Kassiba A. Silver metallic nanoparticles with surface plasmon resonance: synthesis and characterizations. *Journal of Cluster Science.* 2017;28:1051-1069. https://doi.org/10.1007/s10876-016-1080-1
21. Francesko A, Cano Fossas M, Petkova P, Fernandes MM, Mendoza E, Tzanov T. Sonochemical synthesis and stabilization of concentrated antimicrobial silver-chitosan nanoparticle dispersions. *Journal of Applied Polymer Science.* 2017;134(30):45136.

https://doi.org/10.1002/app.45136
22. Dara PK, Mahadevan R, Digita P, Anandan R, Visnuvinayagam S, Kumar LRG, Mathew S, Ravishankar CN. Synthesis and biochemical characterization of silver nanoparticles grafted chitosan (Chi-Ag-NPs): In vitro studies on antioxidant and antibacterial applications. *SN Applied Sciences.* 2020;2:1-12. https://doi.org/10.1007/s42452-020-2261-y
23. Deshmukh AR, Gupta A, Kim BS. Ultrasound assisted green synthesis of silver and iron oxide nanoparticles using fenugreek seed extract and their enhanced antibacterial and antioxidant activities. *BioMed research international.* 2019:1714358. doi: 10.1155/2019/1714358
24. Shah A, Hussain I, Murtaza G. Chemical synthesis and characterization of chitosan/silver nanocomposites films and their potential antibacterial activity. *International journal of biological macromolecules.* 2018;116:520-529. https://doi.org/10.1016/j.ijbiomac.2018.05.057
25. González-Campos JB, Mota-Morales JD, Kumar S, Zárate-Trivino D, Hernández-Iturriaga M, Prokhorov Y, Lepe MV, Garcia-Carvajal Z, Sanchez IC, Luna-Bárcenas G. New insights into the bactericidal activity of chitosan-Ag bionanocomposite: the role of the electrical conductivity. *Colloids and Surfaces B: Biointerfaces.* 2013;111:741-746. https://doi.org/10.1016/j.colsurfb.2013.07.003
26. Ul-Islam M, Alabbosh KF, Manan S, Khan S, Ahmad F, Ullah MW. Chitosan-based nanostructured biomaterials: Synthesis, properties, and biomedical applications. *Advanced Industrial and Engineering Polymer Research.* 2023. doi: 10.1016/j.aiepr.2023.07.002
27. Fatima F, Siddiqui S, Khan WA. Nanoparticles as novel emerging therapeutic antibacterial agents in the antibiotics resistant era. *Biological Trace Element Research.* 2021;199(7):2552-2564. doi: 10.1007/s12011-020-02394-3
28. Waktole G. Toxicity and Molecular Mechanisms of Actions of Silver Nanoparticles. *Journal of Biomaterials and Nanobiotechnology.* 2023;14(3):53-70. doi: 10.4236/jbnb.2023.143005